Invited Paper https://doi.org/10.7733/jnfcwt.2020.18.4.421

Assessment on Recovery of Cesium, Strontium, and Barium From Eutectic LiCl-KCl Salt With Liquid Bismuth System

Michael E. Woods and Supathorn Phongikaroon*
Virginia Commonwealth University, 401 W Main St, Richmond, VA 23284, USA

(Received September 14, 2020 / Revised October 7, 2020 / Approved November 19, 2020)

This study provides an assessment on a proposed method for separation of cesium, strontium, and barium using electrochemical reduction at a liquid bismuth cathode in LiCl-KCl eutectic salt, investigated via cyclic voltammetry (CV), electrochemical impedance spectroscopy (EIS), and scanning electron microscopy with energy dispersive X-ray spectrometry (SEM-EDS). CV studies were performed at temperatures of 723-823 K and concentrations of the target species up to 4.0wt%. Redox reactions occurring during potential sweeps were observed. Concentration of $BaCl_2$ in the salt did not seem to influence the diffusivity in the studied concentration range up to 4.0wt%. The presence of strontium in the system affected the redox reaction of lithium; however, there were no distinguishable redox peaks that could be measured. Impedance spectra obtained from EIS methods were used to calculate the exchange current densities of the electroactive active redox couple at the bismuth cathode. Results show the rate-controlling step in deposition to be the mass transport of Cs^+ ions from the bulk salt to the cathode surface layer. Results from SEM-EDS suggest that Cs-Bi and Sr-Bi intermetallics from LiCl-KCl salt are not thermodynamically favorable.

Keywords: Liquid bismuth cathode, Electrochemical impedance spectxoscopy, Electrochemistry, Cesium, Strontium, Barium

*Corresponding Author.
Supathorn Phongikaroon, Virginia Commonwealth University, E-mail: sphongikaroon@vcu.edu, Tel: +1-804-827-2278

ORCID
Michael E. Woods http://orcid.org/0000-0001-8685-6026 Supathorn Phongikaroon http://orcid.org/0000-0002-2019-0118

1. Introduction

During pyroprocessing of used nuclear fuel (UNF), fission products in the electrorefiner (ER) salts accumulate and degrade the efficiency of the ER by decreasing the electrode reaction, which is uranium capture. This necessitates a cleaning or replacement process of the salts. Furthermore, removal from the salt of the radioactive fission products, especially the short-lived isotopes like ^{137}Cs (half-life of 30.17 y) and ^{90}Sr (half-life of 28.8 y) can lessen the radioactivity of the bulk salt and make shielding and handling easier. The separation of specific fission products from these salts has been the focus of much research and many different techniques, primarily ion exchange [1-3] and zone freezing [4-7].

Although these separation processes successfully demonstrated the recovery of fission products, there is not yet a well-demonstrated technique for the electrochemical separation of other fission products, such as cesium, strontium, and barium. Similar to the way uranium and other actinides can be recovered by the liquid cadmium cathode because of a shift in reduction potentials of the elements for a cadmium cathode, a liquid bismuth cathode (LBC) might be able to be used to capture those fission productions [8, 9]. Furthermore, there is lack of knowledge for electrochemical properties of alkali/alkaline-earths in the eutectic lithium chloride-potassium chloride salt with liquid bismuth (LiCl-KCl/Bi) system. A more robust base of electrochemical knowledge is necessary to confidently assess the potential for application of the liquid bismuth cathode in pyroprocessing technology. These reasons form the motivation for this study to focus on providing a fundamental assessment on electrochemical and kinetics data for representative alkali/alkaline-earth elements (that is, cesium, strontium, and barium) in the LiCl-KCl/Bi cathode system. This data can then be used to make a preliminary decision on the feasibility and performance of the LBC if added to a pyroprocessing scheme. This work was performed via bench-top experiments replicating the ER environment. Electrochemical experiments made use of cyclic voltammetry (CV), electrochemical impedance spectroscopy (EIS), and open circuit potential (OCP) techniques to determine values for important parameters of the process, including redox potentials, diffusivity, and exchange current density of the ions if possible. Recovery of these fission products was analyzed and evaluated by inductively coupled plasma mass spectrometry (ICP-MS) and scanning electron microscopy with energy dispersive spectrometry (SEM-EDS).

2. Theory

2.1 Electrochemical Concept

The electrochemical cell of interest in this study is an electrolytic cell, which consists of two electrodes-a cathode where species are reduced and an anode where species are oxidized-and an electrolyte-a solution or sometimes solid which the electrodes are in contact with and which mediates the movement of ions to the electrode surface. When no external current is applied to the cell, the concentrations of the ions are in equilibrium and the cell will possess a potential referred to as the equilibrium potential $E^{eq}_{M^{n+}/M}$. For an oxidation-reduction reaction which occurs in the cell, its equilibrium potential is described by the Nernst equation,

$$E^{eq}_{M^{n+}/M} = E^{0}_{M^{n+}/M} + \frac{RT}{nF}\ln\left(\frac{a_{M^{n+}}}{a_M}\right) \quad (1)$$

where $E^{eq}_{M^{n+}/M}$ is the standard reduction potential, which is the theoretical potential when the cell is reversible at an equilibrium state and the solution concentration is 1 mol·L^{-1} at 1 atm and 298 K, R is the universal gas constant (8.314 J $mol^{-1}\cdot K^{-1}$), T is the absolute temperature (K), n is the number of electrons transferred, F is Faraday's constant (96,485 C·mol^{-1}), and a_i is the activity of the species. For the LBC system, the binary system of bismuth with the reduced cation is of interest. Eq. (1) can be expressed with respect to this reaction and the activity of the binary system as,

Table 1. Overview of thermodynamic properties of LiCl-KCl/Bi system species and calculated reduction potential shifts at 773 K [10]

M^{n+}/M	E^0 (V) vs Cl^-/Cl_2 (g)	$-\frac{RT}{nF}\ln\left(\frac{a_{M(in\ Bi)}}{a_{M^{n+}}}\right)$ $\chi_{M(in\cdot Bi)} = 0.05$	Ee_q (V) vs Cl^-/Cl_2 (g)
Li^+/Li	-3.550	0.924	-2.626
K^+/K	-3.690	0.967	-2.723
Sr^{2+}/Sr	-3.623	1.004	-2.619
Ba^{2+}/Ba	-3.755	1.164	-2.591

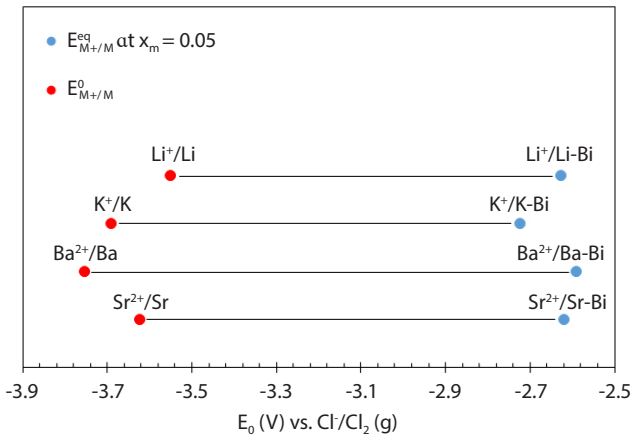

Fig. 1. Graphical depiction of standard reduction potentials (E_0) and shifted equilibrium potentials in liquid bismuth (E^{eq}) based on literature [10].

$$E^{eq}_{M^{n+}/M} = E^0_{M^{n+}/M} - \frac{RT}{nF}\ln\left(\frac{a_{M(in\ Bi)}}{a_{M^{n+}}}\right) \quad (2)$$

With this relation in mind, the shift of reduction potentials with a bismuth cathode due to the low activities of alkali/alkaline-earth species in bismuth can be explained. The electromotive force (emf) technique can be applied to measure and give a value for the second term in the right-hand side of Eq. (2). Using the values for this term of lithium, potassium, strontium, and barium in bismuth that have been measured and reported in literature [8, 9], it is possible to calculate the shifted equilibrium potential of each species in bismuth. The values for standard reduction potentials, second term of right-hand side of Eq. (2), and shifted equilibrium potentials for a 5mol% species in bismuth concentration from literature for the relevant species are given in Table 1 and displayed graphically in Fig. 1. Due to the larger second term of right-hand side of Eq. (2) values of strontium and barium compared to lithium and potassium, the reduction potentials of strontium and barium are shifted to more positive values than lithium and potassium. This suggests the ability to reduce strontium and barium into liquid bismuth, with co-deposition of lithium expected due to the small difference of reduction potentials.

2.2 Background Studies

Few studies have focused on the separation of actinides, rare-earth (RE) elements, and alkali/alkaline-earths by thermodynamic or electrochemical reduction techniques into bismuth. This idea is predicated on the idea that bismuth could then be distilled from the cathode leaving behind the recovered material, similar to the cathode distillation already designed in this electrochemical process [11, 12].

Being that the most valuable materials within UNF are the actinides, many studies have investigated these elements for separation ability with the LBC. By a reductive extraction process, uranium, neptunium, plutonium, and americium can be reduced into bismuth comparably to cadmium by addition of lithium, as a reductant [13]. However, there is a significant amount of lithium added to the system and reduced into the liquid bismuth during this process. Toda and co-workers have shown by calculation with thermodynamic parameters that uranium, plutonium, and americium can be favorably separated into bismuth compared to cerium [14]. Another way of reducing actinides into the liquid bismuth

Table 2. Reported diffusion coefficients from literature for alkaline-earth liquid metal studies

Element	Electrolyte	Cathode	T (K)	D ($x10^5$ $cm^2 \cdot s^{-1}$)	Method	Reference
Strontium	KCl	Lead	1073	1.3 ± 0.3	CV conventional	[26]
				1.7 ± 0.2	CV semi-integral	
				1.6 ± 0.2	CV semi- differential	
				1.9 ± 0.7	CP	
				1.46 ± 0.18	CP	
	NaCl-KCl	Lead	1073	1.42	EIS	[30]
		Zinc	1023	1.46 ± 0.18	CP	[25]
Barium	NaCl-KCl	Lead	1000	1.3 ± 0.2	CV conventional	[28]
				1.1 ± 0.3	CV semi-integral	
				1.2 ± 0.3	CV semi-differential	
				1.0 ± 0.2	CP	
				1.08 ± 0.16	CP	
		Zinc	1023	1.08 ± 0.21	CP	[25]

instead of adding a reductant is by electrolysis. Studies of the electrochemical behavior of thorium [15], uranium [16], neptunium [17,18], and plutonium [19] have shown the reduction of actinide ions into a liquid bismuth phase or onto a bismuth film electrode as various intermetallic species. The small activities of actinides in a liquid bismuth phase due to alloy formation lead to a positive shift of the reduction potential; so, these studies have measured the redox potentials along with the diffusion coefficients of the actinide ions in the salt. These studies have shown reversible behavior using the CV technique.

RE elements have similarly been studied for electrochemical separations using liquid bismuth in LiCl-KCl. Kurata et al. have shown that the distribution of trivalent REs compared to uranium is slightly better for bismuth than for cadmium in LiCl-KCl, reporting separation factors of 10^2-10^6 [13]. CV studies of lanthanum, cerium, praseodymium, and terbium have shown quasi-reversible behavior and similar positive potential shifts of RE redox reactions due to a lowered activity of RE in liquid bismuth, owing to formation of intermetallic compounds [20-24]. For cerium, Castrillejo et al. showed the formation of two intermetallic compounds, $CeBi_2$ and CeBi, by emf measurements and reported Gibbs energies of formation at 773 K for these compounds of -218.5 $kJ \cdot mol^{-1}$ and -211.8 $kJ \cdot mol^{-1}$, respectively [21].

Few studies have been done for the separation of alkali/alkaline-earth species from LiCl-KCl via liquid bismuth. For reductive extraction, the favorable reduction of strontium and barium versus uranium by addition of a reductant is lesser for bismuth compared to cadmium, but still very strong with a separation factor of 10^6-10^7 [13]. For reduction by electrolysis, strontium and barium have been separated into the LBC in LiCl-KCl salts by constant current electrolysis with coulombic efficiencies of 63-67% [10]. There was significant deposition of lithium into the liquid bismuth pool; nevertheless, the overall idea of alkali/alkaline-earth separation in LiCl-KCl salts was demonstrated. The electrochemical behaviors and reductions of Sr^{2+}, Cs^+, and Ba^{2+} on a graphite, liquid bismuth, liquid lead, or liquid zinc cathode have been studied in KCl, equimolar NaCl-KCl, or LiCl-$CaCl_2$-NaCl salts, reporting

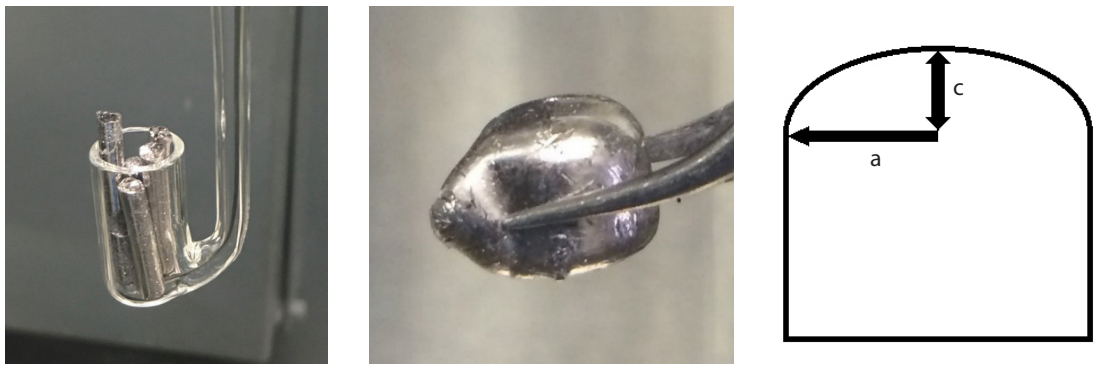

(a) (b) (c)

Fig. 2. (a) Cup-type cathode with bismuth and molybdenum wire connection; (b) bismuth cathode post experiments; and (c) Diagram of measurements for calculation of surface area of bismuth cathode.

quasi-reversible redox reactions and diffusion coefficients [9], [25-30]. The values reported for the diffusion coefficient are presented in Table 2. Since these studies serve as a reference for this project as it fills in the gaps of fundamental knowledge of LiCl-KCl/Bi systems for alkali/alkaline-earth electrochemical separations.

3. Experimental

Anhydrous bead type lithium chloride (LiCl, 99.995%), potassium chloride (KCl, 99.95%), silver chloride (AgCl, 99.997%), strontium chloride ($SrCl_2$, 99.995%), cesium chloride ($CsCl_2$, 99.99%), and barium chloride ($BaCl_2$, 99.998%) were purchased from Alfa Aesar. Salts were prepared under argon inside the glovebox (Innovative Technology with less than 5 ppm of O_2 and H_2O). Alumina crucibles (Al_2O_3, 99.8%) of size 40 mL and 180 mL were purchased from Coorstek. Prior each experiment (outside the glovebox), both crucibles were sonicated in 2% HNO_3 acid with ultrapure water and dried in a benchtop oven at 473 K for 2 hours. Once inside the glovebox, the small crucible was loaded with the LiCl-KCl eutectic (58.2: 41.8mol% composition) and then placed into a large Al_2O_3 crucible-serving as a safety crucible in case of spillage or breakage from the small crucible. These crucibles were then loaded into the furnace (Thermo Scientific) and heated at 573 K for 5 hours minimum to further dry out and outgas the salts and crucibles. After this drying process, the salts were raised to the beginning experimental temperature, typically 723 K, and allowed to melt and equilibrate for a minimum 2 hours before electrodes or other salts were added. At least a 24-hour period was allowed for dissolution and for the system to reach equilibrium prior running electrochemical experiments.

Two different types of LBC were studied, (1) a pool-type and (2) a cup-type. Bismuth needles (99.99%) were purchased from Alfa Aesar. To remove oxides and obtain a pure bismuth metal, the bismuth needles were melted in the furnace inside the glovebox in a 40 mL alumina crucible at 673 K. A Pyrex tube with inner diameter 2 mm was dipped into the bismuth metal below the oxidation and a connected syringe used to draw bismuth metal up into the tube. This recovered a pure bismuth metal with no visible oxidation. The Pyrex tube was then broken open and the new bismuth needles recovered for use in experiments.

For the cup-type cathode, a custom-made Pyrex electrode from a local glass shop, Research Glass, was used and is shown in Fig. 2(a). The shaft was 7 mm and open to the attached bottom. (a) 0.5 mm molybdenum wire was threaded through the tube and into the bottom cup before addition of approximately 5 g of bismuth needles to the cup.

Details will be discussed later.

For the pool-type cathode, bismuth needles were added to a 40 mL crucible before addition of the salts and melted at 773 K for 1 hour in the glovebox furnace. After visual confirmation of the liquid bismuth phase, the system was cooled to room temperature and the LiCl-KCl were added. In one study performed, a 10mol% barium in bismuth cathode was made. This was done by adding barium metal (99.9%) acquired from Alfa Aesar to purified bismuth needles and melting at 798 K in the 40 mL crucible. The liquidus point for 10mol% barium in bismuth is approximately 645 K [31]. Needles of this Ba-Bi alloy were then extracted via a 2 mm inner diameter Pyrex tube and syringe in a process similar to the pure bismuth needle preparation. Then, the Ba-Bi needles were loaded into a 40 mL crucible and prepared as a pool-type cathode in the same method as for pure bismuth. For both the Ba-Bi and the bismuth pool-type cathodes, a tungsten rod of diameter 1.5 mm (99.95%) purchased from Alfa Aesar was sheathed with an alumina tube and used to make contact with the liquid metal pool. The surface area of the bismuth cathode was measured after each experimental run.

The Pyrex cup was broken open and the bismuth cathode extracted. Minimal adhesion of the salt to the bismuth allowed for a clean extraction. The bismuth cathode post-experiments is shown in Fig. 2(b). The surface area of the top bismuth surface was calculated by using the formula for surface area of an oblate spheroid and multiplying by half to get the surface area of the half spheroid [32],

$$S = \pi a^2\left(1 + \frac{(c/a)^2}{2\sqrt{1-(c/a)^2}}\ln\left(\frac{1+\sqrt{1-(c/a)^2}}{1-\sqrt{1-(c/a)^2}}\right)\right) \quad (3)$$

where the parameters a and c are the diameter and height of the half-spheroid, respectively, as shown in Fig. 2(c).

All experiments were performed using a Ag/AgCl reference electrode (RE) (5mol% AgCl in LiCl-KCl). The housing of the electrode was custom made by Research Glass and consisted of a 7 mm outer diameter Pyrex tube open on one end and on the other closed with a thin wall less than 0.5 mm in thickness. The thin surface allows ionic conduction between the bulk electrolyte and reference electrolyte. A 1 mm Ag wire (99.99%) purchased from Alfa Aesar was inserted into the tube with the bottom end submerged in the salts approximately 5 mm from the thin bottom surface and the top end protruding out of the top allowing connection to the potentiostat.

A three-electrode system was used for all experiments similar to a study by Yoon et al. (see Fig. 3) [33]. The Bi cup-type or pool-type cathode was used as a working electrode (WE). Here, the counter electrode (CE), a 3-mm diameter glassy carbon rod purchased from HTW, was housed in an alumina sheath to insulate it from the steel electrode assembly. A K-type thermocouple probe (Omega Instruments) was sheathed in an 8 mm outer diameter (99.8% alumina from Coorstek), contacting with the salt. These items were held in place by a custom-made steel electrode assembly at the top of the furnace.

All electrochemical measurements were completed by using a Biologic Science Instruments VSP-300 potentiostat/galvanostat. Data sets were collected and analyzed by Biologic Science Instrument EC-Lab V11.20. Table 3 shows a summary of the experimental program and detailed parameters. Only one element was studied in each experimental run. Likewise, CV and EIS experiments were always performed in separate experimental runs.

Many of the electrochemical experiments performed aimed to measure the properties of salt species at varying concentrations. In order to verify salt species concentrations, salt samples withdrawn during experiments were analyzed by ICP-MS (Agilent Scientific Instruments 7900). Analytical routine of these salts was similar to those reported by previous study [33]. Furthermore, to characterize the bismuth cathodes after electrochemical experiments, an SEM-EDS (Phenom ProX Desktop) was utilized. Here, the cathode is first visually scanned by the SEM user for visible heterogeneity in the sample, indicating the presence of multiple phases of material. These are usually apparent as darker and lighter patches within the cross section. When

Table 3. Summary of experimental program

	Experimental Run				
	1	2	3	4	5
Salt Species	CsCl	CsCl	$SrCl_2$	$BaCl_2$	$BaCl_2$
Concentration (wt% in LiCl-KCl)	0.5, 1.0, 1.5, 2.0, 3.0, 4.0	0.5	0.5, 1.0, 1.5, 2.0, 3.0, 4.0	0.5, 1.0, 1.5, 2.0, 2.5, 3.0, 3.5, 4.0	0.78, 1.5, 3.0
Cathode Type	Bi Cup	Bi Pool	Bi Cup	Bi Cup	Ba-Bi Pool
Electrochemical Method	CV	EIS	CV	CV	EIS
Temperature (K)	723, 748, 773, 798, 823	723, 748, 773	723, 748, 773, 798, 823	723, 748, 773, 798, 823	723, 748, 773, 798, 823
Electrical Potential Range (V)	0.3 to -1.55	-	0.22 to -1.55	0.3 to -1.5	-
Scan rate ($mV \cdot s^{-1}$)	50, 100, 150, 200	-	25, 50, 75, 100, 150, 200	50, 100, 150, 200	-
Potential Amplitude (mV)	-	10	-	-	10
Frequency Range	-	50 kHz – 10 mHz	-	-	50 kHz - 50 mHz
Bi Surface Area (cm^2)	0.743	5.26	0.750	0.776	8.40

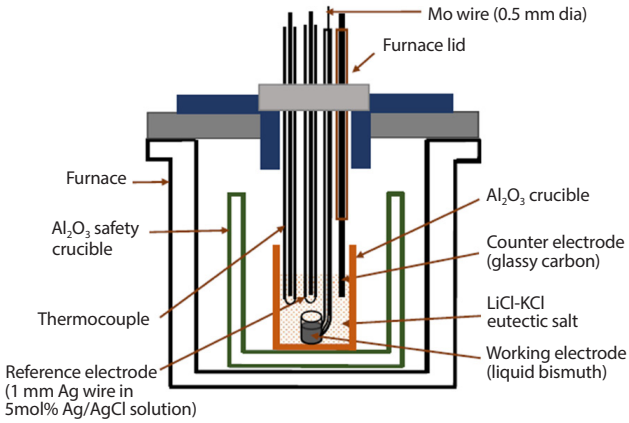

Fig. 3. Diagram of electrode assembly and furnace.

these patches are discovered, the SEM user selects these as target spots for EDS analysis. The Phenom ProX uses 15 kV X-rays to probe the target spot for a period of 90 seconds while it collects spectroscopic information. The software then returns results to the user as a plot of spectral counts and calculated elemental compositions as atomic and weight percentages.

4. Results and Discussion

4.1 CV Measurements

Pure LiCl-KCl cyclic voltammograms were obtained at each temperature and scan rate before additions of CsCl, $SrCl_2$ or $BaCl_2$. This allowed for a subtraction method to be applied to obtain voltammograms relating only to the reactions of the interested species. An example of these voltammograms and subtraction method is shown in Fig. 4(a) for the system with 4wt% CsCl at 773 K and 100 $mV \cdot s^{-1}$ scan rate. Subtraction voltammograms representative of the CsCl-LiCl-KCl system on the LBC are shown in Fig. 4(b). At the positive end, the reduction occurring at -0.13 V is attributable to free bismuth in the system. This behavior was seen during all CV experiments with the LBC. The final rise occurring at the positive end of the anodic scan corresponds to the anodic dissolution of bismuth from the cathode. Likewise, the strong reduction occurring at

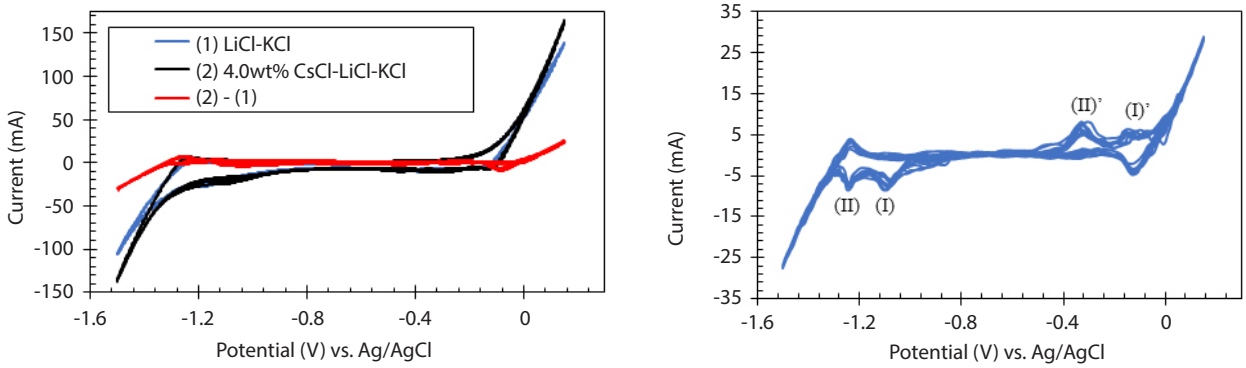

(a) (b)

Fig. 4. (a) Cyclic voltammogram of pure LiCl-KCl, 4wt% CsCl-LiCl-KCl, and subtraction at 773 K and scan rate 100 mV·s^{-1}; (b) Subtraction cyclic voltammograms for the 0.5wt% CsCl-LiCl-KCl system at 823 K and scan rate 100 mV·s^{-1}. WE: bismuth (surface area: 0.743 cm^2), CE: glassy carbon, RE: Ag/AgCl.

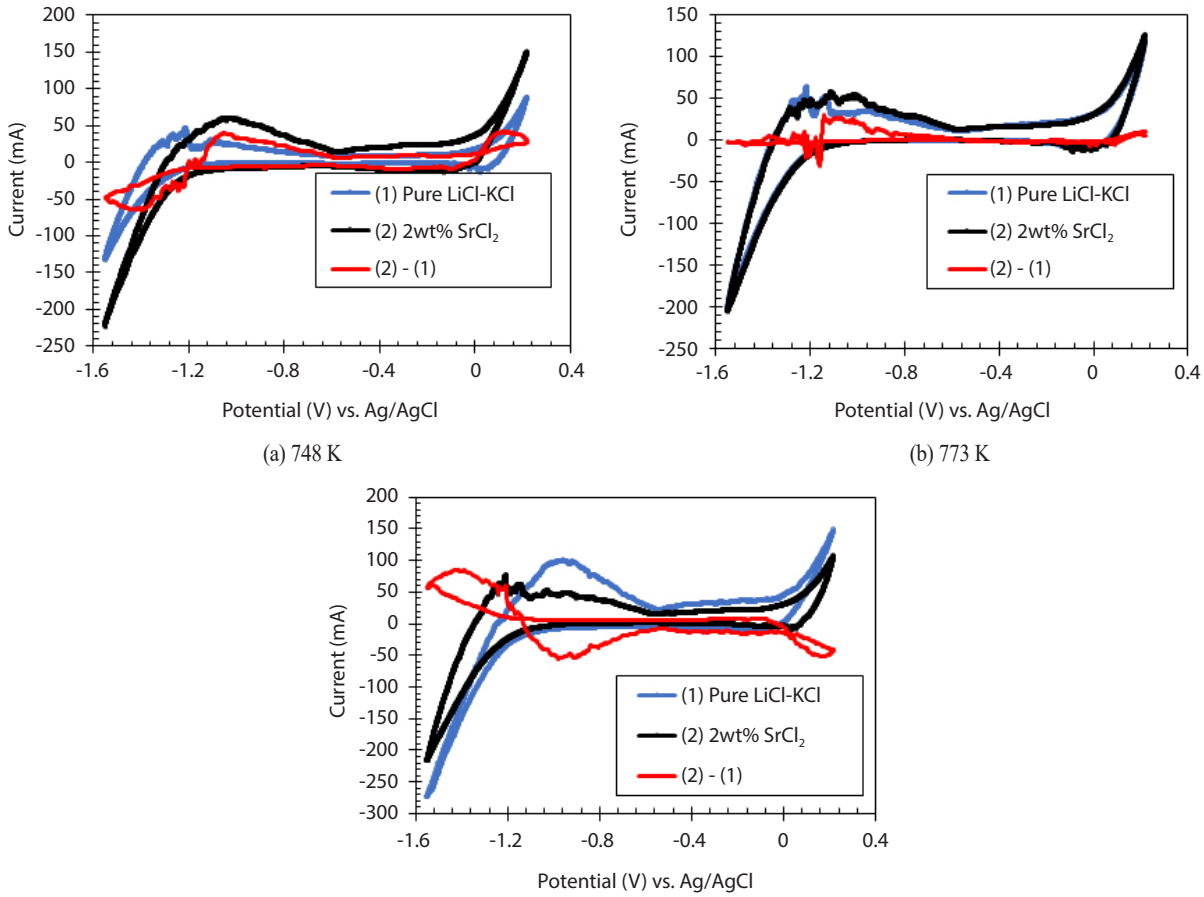

(a) 748 K (b) 773 K

(c) 798 K

Fig. 5. Cyclic voltammograms and background LiCl-KCl subtraction curve for 2wt% $SrCl_2$-LiCl-KCl system at a scan rate of 25 mV·s^{-1} and temperature of (a) 748 K, (b) 773 K, and (c) 798 K. WE: bismuth (surface area: 0.750 cm^2), CE: glassy carbon, RE: Ag/AgCl.

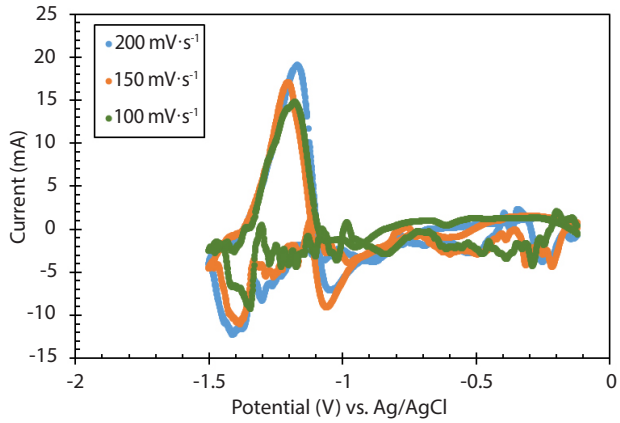

Fig. 6. Subtracted CV curves for 1wt% $BaCl_2$ system at 798 K. WE: bismuth (surface area: 0.776 cm^2), CE: glassy carbon, RE: Ag/AgCl.

the negative end of the cathodic scan is attributable to the reduction of a Li-Bi alloy in the system, as many other researchers have likewise discovered [19, 20, 23]. The two redox reactions of interest attributable to the presence of cesium occur with (I) reduction at -1.1 V and oxidation at -0.15 V, and (II) reduction at -1.24 V and oxidation at -0.32 V. The peak potentials moved slightly in the negative direction with increasing scan rate. Thus, the reaction might be quasi-reversible as it is extremely difficult to determine. Additionally, the difference in CV scans could be the result of a changing surface area of the working electrode.

For the strontium experiments, a potential range of 0.22 to -1.55 V was shown to produce repeatable CV curves, exhibiting behavior similar to the cesium studies. After subtraction of the background current (see Fig. 5), assuming the subtraction is not just insignificant noise, we see that the presence of $SrCl_2$ causes a large variation in the reduction of lithium at the negative end of the potential range. At 773 K, the lithium reduction for the system, which contains $SrCl_2$, occurs with approximately equivalent current-potential characteristics as the pure LiCl-KCl system. However, the presence of $SrCl_2$ seems to decrease the effect of temperature on the lithium reduction. In the pure LiCl-KCl system, the current peaks at the end of the potential sweep (E = -1.55 V) vary by about 50 mA for each 25 K temperature difference. However, in the 2wt% $SrCl_2$-LiCl-KCl system, there is no apparent variation of the reduction current-potential relationship with respect to temperature.

Fig. 6 shows the sample CV curves after subtraction of the background current for the $BaCl_2$-LiCl-KCl system. A redox reaction is seen with a reduction peak at approximately -1.40 V and an oxidation peak at roughly -1.27 V. Here, for the $BaCl_2$ system, the only CV studies with repeatable CV curves came from the systems containing 1wt% or 2wt% $BaCl_2$. From the curves with prominent redox peaks in these systems, the anodic peaks of the redox reaction were then measured.

Based on the representative CV plots, it was not possible to extract the diffusion values for cesium, strontium and barium data sets. Although Lichtenstein and coworkers [10] have report their successful deposition of strontium and barium into a bismuth cathode by cathodic discharge, their experimental setup were set as separated compartments similar to battery cell system. That is, their systems are different from our current systems of no barriers between the electrodes and salt medium.

4.2 EIS Measurements

EIS experiments were selected and conducted for a CsCl-LiCl-KCl and $BaCl_2$-LiCl-KCl systems on a bismuth pool-type electrode. In principal, we would like to determine whether it was possible to extract these elements with larger metallic pool surface; this would also allow us to determine the exchange current density i_0 of the Cs^+/Cs and Ba^{2+}/Ba redox couples on the bismuth interface.

Fig. 7 shows representative impedance spectra for the 0.5wt% CsCl-LiCl-KCl system at 773 K where the applied potential was increased beyond the equilibrium potential by steps of 1 mV. EIS is ideally performed at the equilibrium potential for calculation of the exchange current density (i_0). Fig. 7 illustrates that the impedance increases dramatically at high frequencies; at low frequencies, there is no ion transfer occurring between the bismuth and cesium ions. Thus, small overpotentials were applied to the system to

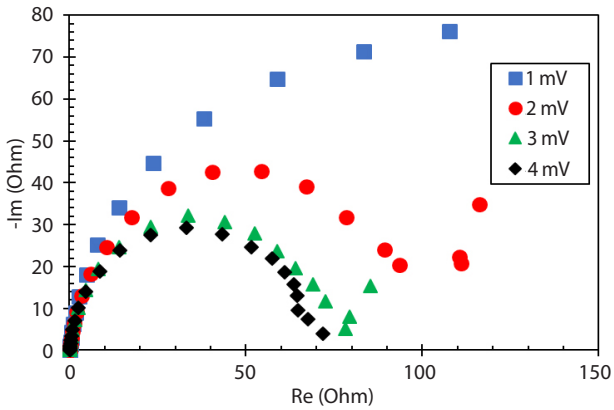

Fig. 7. Nyquist plot for 0.5wt% CsCl-LiCl-KCl system at 773 K on a pool-type bismuth cathode (surface area: 5.26 cm^2).

initiate Cs^+ reduction at the bismuth cathode. Here, the applied overpotential is increased to 2 mV, a diffusion related resistance starts to occur at the low frequencies. This indicates that there is electron transfer at the cathode surface and that the diffusion of Cs^+ ions from the bulk salt to the electrode surface is occurring. Overpotentials were found by this procedure at each experimental temperature and these Nyquist plots were used to fit to an equivalent circuit for calculation of the charge transfer resistance Rct.

For the barium experiments, a pool-type bismuth cathode containing 10mol% barium was used. Moreover, the working area of the bismuth cathode via pool-type cathode was chosen for a better EIS measurement. The Nyquist plots were following similar shapes and patterns of those from the cesium studies. The Nyquist plots generated by EIS techniques can be fitted to an equation of an equivalent circuit for modeling the system. A proposed circuit for this system is displayed in Fig. 8(a)-composed of the bulk solution resistance, a double layer capacitance at the cathode surface, the charge transfer resistance, and the Warburg diffusion related resistance. This circuit can be represented by the Voigt model for an electrode process, for which the impedance is expressed by the following equation [34].

$$Z(t) = R_s + \frac{1}{\frac{1}{R_{ct}} + \frac{1}{W} + j\omega C_{dl}} = R_s + \frac{1}{1 + \frac{R_{ct}}{W} + j\omega R_{ct} C_{dl}} \quad (4)$$

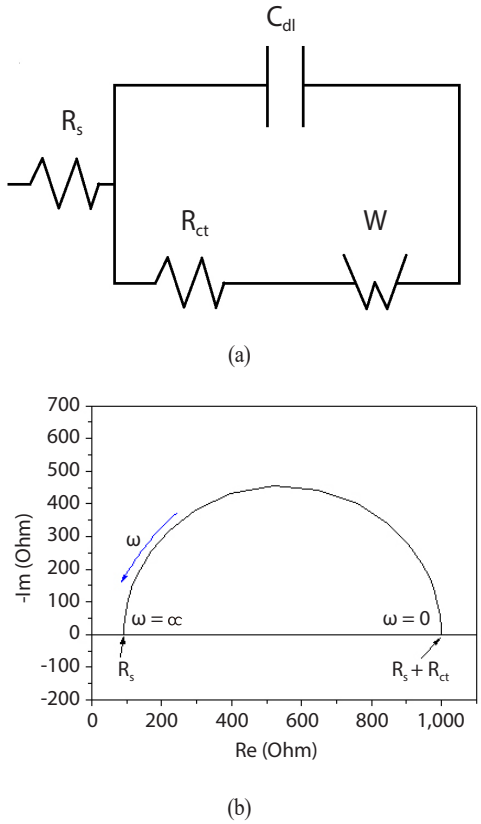

Fig. 8. (a) Equivalent circuit for the liquid bismuth cathode electrochemical cell, including bulk solution resistance R_s, capacitance of the double layer at the cathode surface C_{dl}, charge transfer resistance R_{ct}, and the Warburg diffusion related resistance W;
(b) The ideal Nyquist plot for the Voigt model, showing how the solution resistance R_s and charge transfer resistance R_{ct} can be read and calculated from the x-axis intercepts [34].

To simplify the circuit, a constant phase element can be introduced which represents the Warburg impedance and the double layer capacitance. A constant phase element (CPE) is useful in fitting equivalent circuits because it can represent a resistor, inductor, capacitor, Warburg response, or a combination of these impedances. The impedance of a CPE can be expressed as [33, 35].

$$Z_{CPE}(\omega) = \frac{1}{(j\omega)^{\alpha} Q} \quad (5)$$

where Q is the capacitance and α is an exponent that is less than or equal to one. Upon inspection of Eq. (6), the second

Table 4. Reporting η, R_{ct} × S, and i_0 values at different temperatures for 0.5wt% CsCl system

T (K)	η (mV)	R_ct×S (Ω cm^2)	i_0 (A cm^{-2})
723	2	0.828	0.0752
748	2	0.739	0.0843
773	2	0.684	0.0911

Table 5. Measured R_{ct} × S and calculated i_0 values for the Ba^{2+}/Ba reaction on the liquid bismuth cathode by EIS technique

T (K)	0.78wt% $BaCl_2$		1.5wt% $BaCl_2$		3.0wt% $BaCl_2$	
	R_{ct}×S (Ω cm^2)	i_0 (A cm^{-2})	R_{ct}×S (Ω cm^2)	i_0 (A cm^{-2})	R_{ct}×S (Ω cm^2)	i_0 (A cm^{-2})
723	0.535	0.0583	0.569	0.0550	0.564	0.0553
748	0.453	0.0716	0.501	0.0655	0.492	0.0655
773	0.422	0.0790	0.463	0.0743	0.461	0.0723
798	0.395	0.0894	0.437	0.0796	0.413	0.0832
823	0.316	0.118	0.311	0.121	-	-

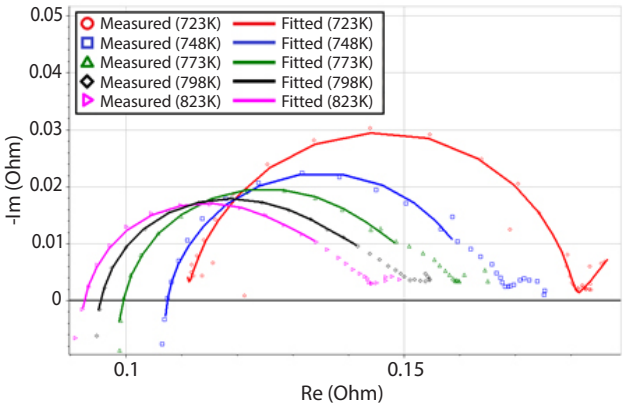

Fig. 9. Measured and fitted impedance spectra for the LiCl-KCl system with 0.78wt% $BaCl_2$ at temperatures of 723-823 K on the pool-type Ba-Bi cathode (surface area: 8.40 cm^2).

term of the impedance relation is negligible at very high frequency whereas the second term approaches R_{ct} when the frequency is low. Fig. 8(b) shows an ideal Nyquist plot for the Voigt model, where R_s and R_s+R_{ct} are easy to find on the x-axis [34].

The charge transfer resistance is relevant to the redox reaction occurring at the cathode surface, and allows for calculation of the exchange current density according to the following equation [36].

$$R_{ct} = \frac{RT}{nFi_0} \quad (6)$$

The impedance spectra were first automatically fitted by the Z-fit software from Biologic Scientific Instruments. Then, the fit was manually adjusted by changing the values of some of the equivalent circuit components. This was performed to minimize the relative error to a value below 0.10. The curve was then used to provide a value for the product of Rct and the surface area of the cathode in the system. From these values, i_0 on the Bi cathode was tabulated. Fig. 9 shows the measured and fitted impedance spectra for the Ba experiments (0.78wt% $BaCl_2$).

Table 4 gives the values of R_{ct}×S and i_0 collected from the fits of the impedance spectra for the CsCl containing system. When these values for exchange current density and diffusion coefficient are compared with each other and to other similar systems, it can be seen that the exchange current mechanism is much less likely to be the rate-controlling step in deposition than the mass transport of Cs^+ ions from the bulk salt to the cathode surface layer. Table 5 lists the experimentally attained R_{ct}×S and i_0 values for the barium studies. The results show that the exchange current density

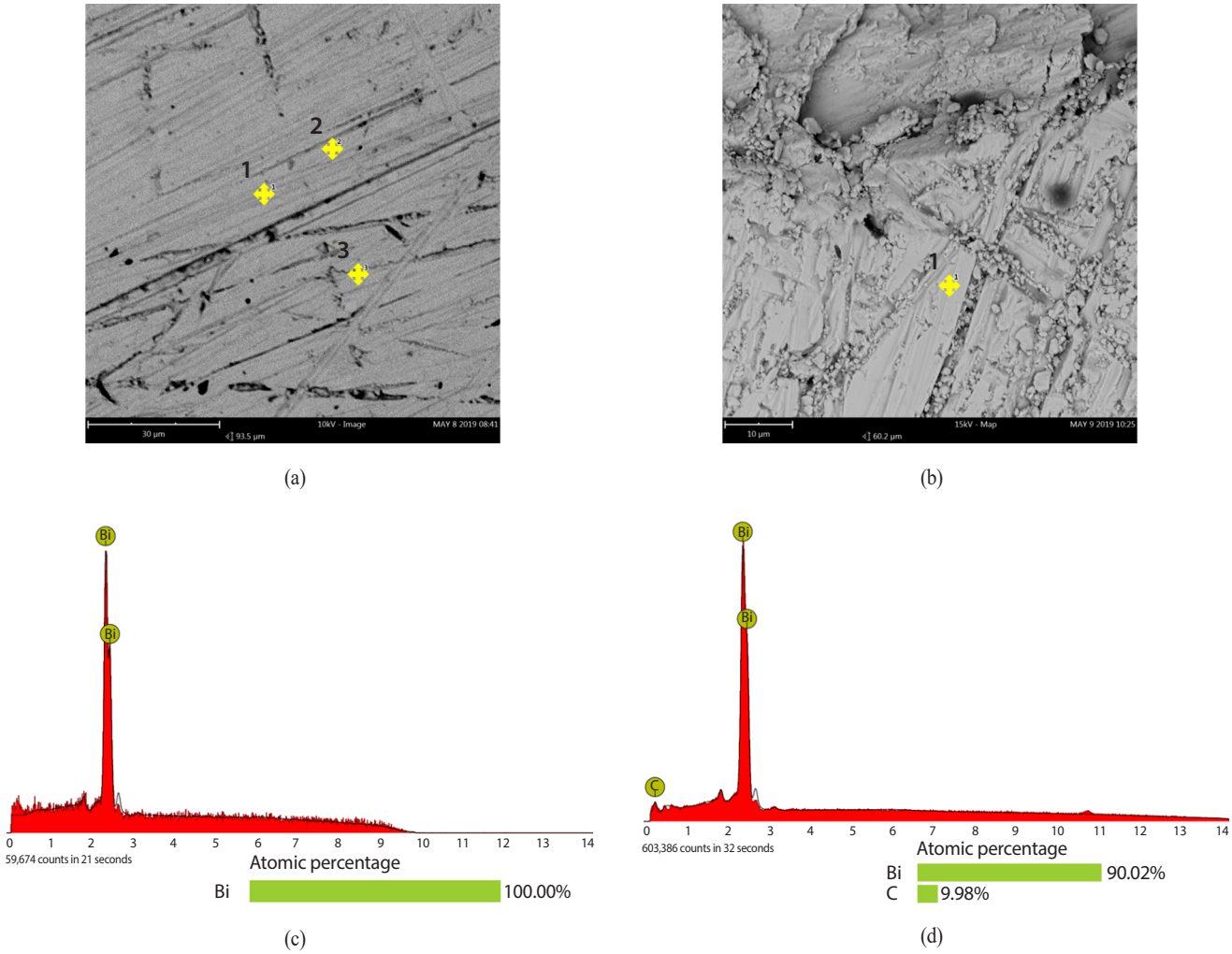

Fig. 10. SEM images of bismuth cathode in CsCl-LiCl-KCl system used in (a) CV and (b) EIS studies. EDS analysis of bismuth cathode of spot 1 for (c) CV and (d) EIS.

ranges from 0.055~0.0583 A cm^{-2} at 723 K to 0.118~0.121 A cm^{-2} at 823 K and does not vary much with increasing concentration of $BaCl_2$ in the salt. The magnitude of these i_0 values obtained by EIS are comparable to values obtained by Yoon and coworkers [33] for the Ce^{3+}/Ce reaction on a liquid cadmium cathode.

4.3 SEM/EDS Analyses

After electrochemical experiments, all used bismuth cathodes were collected and prepared for the SEM-EDS analysis. Analysis of both cathodes types for CsCl-LiCl-KCl/Bi systems yielded no evidence of Cs-Bi intermetallics present. Fig. 10(a) and 10(b) show SEM images of the cathode cross section analyzed from the bismuth Cathode for CV and EIS experiments, respectively. The target spots are labelled on Fig. 10(a) and Fig. 10(c) display the EDS elemental composition analysis of that target spot 1, which suggests 100% Bi present. Fig. 10(d) shows the EDS analysis of the target spot for Fig. 10(b) suggesting 90.02% Bi composition. Here, the measurement of carbon was suspected to be an outliner; overall, the results suggests that

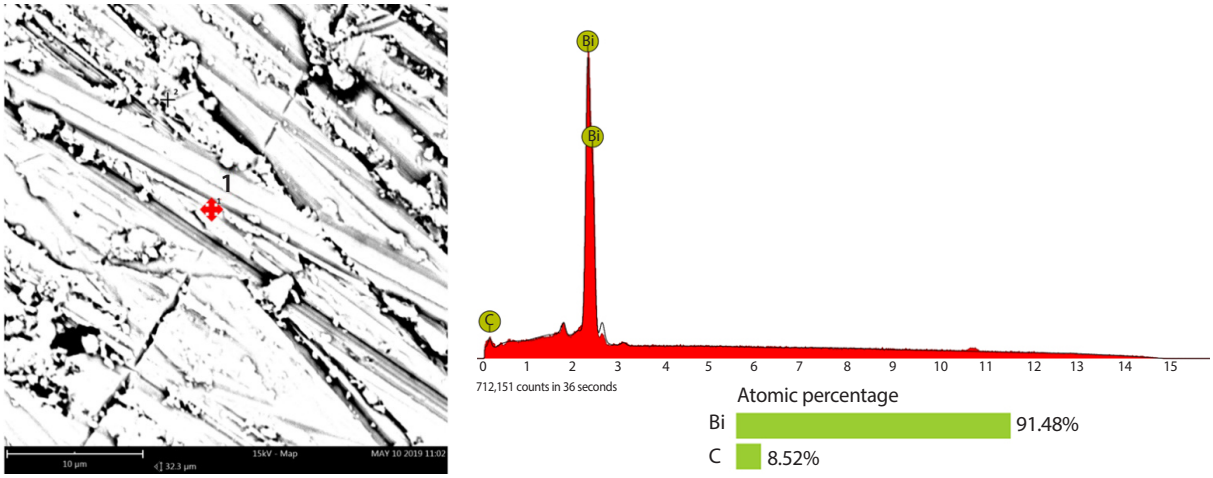

(a) (b)

Fig. 11. (a) SEM image of bismuth cathode used in CV studies of $SrCl_2$; (b) EDS analysis of spot 1.

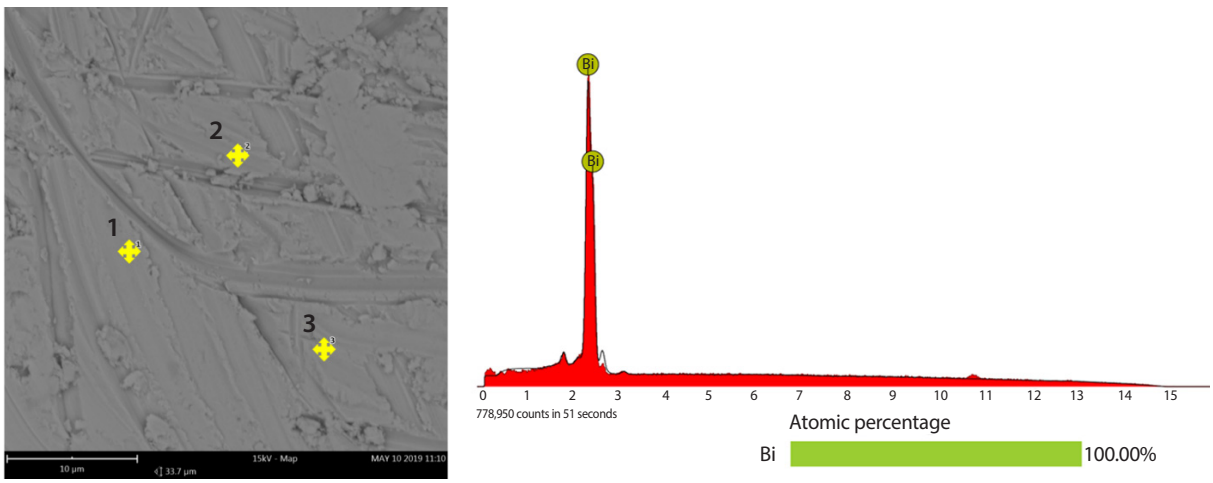

(a) (b)

Fig. 12. (a) SEM image of bismuth cathode used in CV studies of $BaCl_2$; (b) EDS analysis of spot 1.

cesium does not become an alloy thermodynamically in the CsCl-LiCl-KCl/Bi system.

For strontium experiments, multiple image shots of bismuth cathode were taken with EDS analysis in order to confirm or otherwise reject the presence of Sr-Bi intermetallics in the cathode. Fig. 11(a) shows an image from the SEM analysis of the cathode cross section with target shots for EDS analysis labelled. Visual inspection of the cathode cross section yielded no visible phases of Sr-Bi intermetallics, which was confirmed by EDS analysis of the labelled target shots. Fig. 11(b) shows the EDS results of target shot 1, indicating only the presence of bismuth and the absence of Sr-Bi intermetallics. Although Lichtenstein and coworkers [10] have discovered Sr-Bi intermetallics in a bismuth cathode subjected to cathodic discharge in a $SrCl_2$-LiCl-KCl system, in our current study, we found no

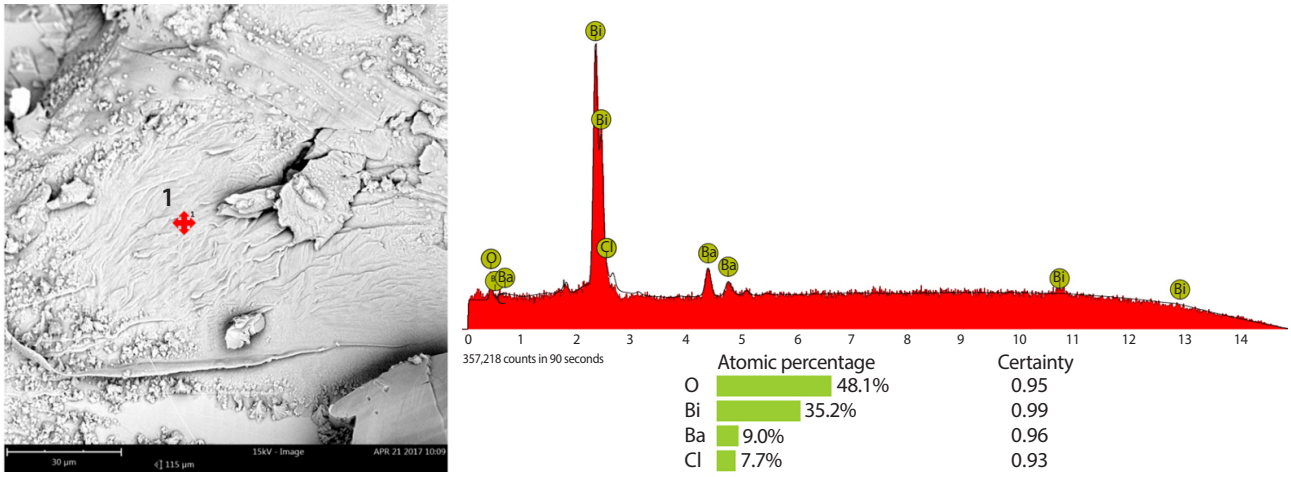

(a) (b)

Fig. 13. (a) SEM image of Ba-Bi cathode used in EIS studies of $BaCl_2$; (b) EDS analysis of spot 1.

Sr-Bi intermetallics present by SEM-EDS analysis. Since the current study was performed with CV analysis, where any reduced strontium species are oxidized from the cathode on the cathodic sweep, Sr-Bi intermetallics should not be expected to be found in the bismuth cathode unless they distribute favorably by thermodynamics. The results of the current study, finding no Sr-Bi intermetallics present in the bismuth cathode, agree well with a study by Kurata and coworkers [13], which found strontium to not distribute thermodynamically into a liquid bismuth pool from LiCl-KCl.

Fig. 12(a) shows an image of the cup-type bismuth cathode used in CV studies of $BaCl_2$. Inspection of the cathode cross section yielded no evidence of visible Ba-Bi intermetallics or other phases, which was confirmed by sampling with EDS analysis. Fig. 12(b) shows EDS analysis of target spot 1 from Fig. 12(a). All three target spots shown in Fig. 12(a), as well as other target spots from the cross section of the cathode, yielded EDS results of 100% Bi composition.

Contrary to the cathode used in CV studies of $BaCl_2$, SEM-EDS study of the Ba-Bi cathode used in EIS studies showed presence of Ba-Bi intermetallics in the cathode cross section. Fig. 13(a) shows an SEM image taken of the cathode cross section with the EDS target spot labelled and Fig. 13(b) shows EDS analysis of the labelled target spot. EDS results showed a significant amount of oxygen present, likely from oxidation of the bismuth surface, as well as the presence of barium in a 9 to 35 atomic ratio to bismuth. This is close to the 31mol% to 69mol% ratio of barium to bismuth reported by Lichtenstein and coworkers for SEM-EDS analysis of a bismuth cathode which has undergone constant current density cathodic discharge in a 5mol% $BaCl_2$-LiCl-KCl system [31]. This comparison suggests presence of the same Ba-Bi intermetallic, likely $BaBi_3$ based on the molar ratio and the Ba-Bi phase diagram, reported by Lichtenstein and co-workers [31].

5. Conclusion

The data and analyses presented in this study have shown electrochemical separation abilities of the liquid bismuth cathode for some of the varied valency elemental species considered with certain conditions. In the case of CsCl, two redox peaks were observed as more positive

than that of lithium, indicating that the controlled deposition of cesium from a CsCl-LiCl-KCl system into the LBC was feasible. However, it should be noted that as diffusion of CsCl in LiCl-KCl was suggested by CV and EIS to be the rate-determining step, the sharp decrease in diffusivity of the CsCl at higher weight percentages meant that the salt recycling process would become less efficient at higher concentrations of CsCl in the ER salt.

For the divalent species studied, strontium and barium, redox reactions were less observable. In the $BaCl_2$ system, weak redox reactions due to $BaCl_2$ were seen to occur at potentials just slightly more positive than the reduction of lithium. From the mass transport and exchange current kinetics values calculated in this study, the reduction of barium into a bismuth cathode should proceed limited by diffusion. In the case of the $SrCl_2$-LiCl-KCl system, no distinguishable redox reaction occurred which could be studied independently of the Li redox. However, from the electrochemical behavior observed, the presence of strontium influences the redox reactions occurring near the reduction potential of Li^+. Although SEM-EDS analysis showed no strontium present in the bismuth cathodes post-examination, it could be possible that as other studies reported, the separation of strontium into bismuth from LiCl-KCl was not thermodynamically favorable. Clearly, Lichtenstein and coworkers [10] showed a possible path of separating strontium into the bismuth cathode from LiCl-KCl. Yet, this study showed that sensitive redox control and electrochemical analysis of the system might not be feasible for selective separation of strontium in the ER salt.

Acknowledgements

This study was performed using two funding sources: (1) The DOE Office of Nuclear Energy's Nuclear Energy University Programs (NEUP) in collaboration with the Pennsylvania State University (NEUP-15-8126) and (2) The Nuclear Regulatory Commission Graduate Student Fellowship received from VCU.

REFERENCES

[1] J.P. Ackerman, T.R. Johnson, and J.J. Laidler, "Waste Removal in Pyrochemical Fuel Processing for the Integral Fast Reactor", Proc. of Int, Symp. on Actinides: Processing & Materials, 1994 TMS Annual Meeting, CA, San Francisco (1994).

[2] Michael F. Simpson. Developments of Spent Nuclear Fuel Pyroprocessing Technology at Idaho National Laboratory, Idaho National Laborator Report, INL/EXT-12-25124 (2012).

[3] M. Shaltry, S. Phongikaroon, and M.F. Simpson, "Ion exchange kinetics of fission products between molten salt and zeolite-A", Microporous Mesoporous Mater., 152, 185-189 (2012).

[4] Y. Cho, G. Park, H. Lee, and I. Kim, "Concentration of Cesium and Strontium Elements Involved in a LiCl Waste Salt by a Melt Crystallization Process", Nucl. Technol., 7(3), 325-334 (2010).

[5] Y.Z. Cho, T.K. Lee, J.H. Choi, H.C. Eun, H.S. Park, and G. Il Park, "Eutectic(LiCl-KCl) waste salt treatment by sequencial separation process", Nucl. Eng. Technol., 45(5), 675-682 (2013).

[6] A.N. Williams, M. Pack, and S. Phongikaroon, "Separation of strontium and cesium from ternary and quaternary lithium chloride-potassium chloride salts via melt crystallization", Nucl. Eng. Technol., 47(7), 867-874 (2015).

[7] M. Shim, H.G. Choi, J.H. Choi, K.W. Yi, and J.H. Lee, "Separation of Cs and Sr from LiCl-KCl eutectic salt via a zone-refining process for pyroprocessing waste salt minimization", J. Nucl. Mater., 491, 9-17 (2017).

[8] J. Serp, P. Lefebvre, R. Malmbeck, J. Rebizant, P. Vallet, and J. P. Glatz, "Separation of plutonium from lanthanum by electrolysis in LiCl-KCl onto molten bismuth electrode", J. Nucl. Mater., 340(2-3), 266-270 (2005).

[9] H. Kim, N. Smith, K. Kumar, and T. Lichtenstein, "Electrochemical Separation of Barium into Liquid Bismuth by Controlling Deposition Potentials", Electrochim. Acta., 220, 237-244 (2016).

[10] T. Lichtenstein, T.P. Nigl, N.D. Smith, and H. Kim, "Electrochemical deposition of alkaline-earth elements (Sr and Ba) from LiCl-KCl-$SrCl_2$-$BaCl_2$ solution using a liquid bismuth electrode", Electrochim. Acta., 281, 810-815 (2018).

[11] B.R. Westphal, J.C. Price, D. Vaden, and R.W. Benedict, "Engineering-scale distillation of cadmium for actinide recovery", J. Alloys Compd., 444-445 (2007).

[12] S. Lee and J. Jang, "Distillation behavior of cadmium for U recovery from liquid cadmium cathode in pyroprocessing", J. Radioanal. Nucl. Chem., 314(1), 491-498 (2017).

[13] M. Kurata, Y. Sakamura, T. Hijikata, and K. Kinoshita, "Distribution behavior of uranium, neptunium, rare-earth elements (Y, La, Ce, Nd, Sm, Eu, Gd) and alkaline-earth metals (Sr, Ba) between molten LiCl-KCI eutectic salt and liquid cadmium or bismuth", J. Nucl. Mater., 227(1-2), 110-121 (1995).

[14] T. Toda, T. Maruyama, K. Moritani, H. Moriyama, and H. Hayashi, "Thermodynamic properties of lanthanides and actinides for reductive extraction of minor actinides", J. Nucl. Sci. Technol., 46(1), 18-25 (2009).

[15] K. Liu, L.Y. Yuan, Y.L. Liu, X.L. Zhao, H. He, G.A. Ye, Z.F. Chai, and W-Q. Shi, "Electrochemical reactions of the Th^{4+}/Th couple on the tungsten, aluminum and bismuth electrodes in chloride molten salt", Electrochim. Acta., 130, 650-659 (2014).

[16] O. Shirai, K. Uozumi, T. Iwai, and Y. Arai, "Electrode reaction of the U^{3+}/U couple at liquid Cd and Bi electrodes in LiCl–KCl eutectic melts", Anal. Sci., 17, i959-i962 (2001).

[17] Y. Sakamura, O. Shirai, T. Iwai, and Y. Suzuki, "Thermodynamics of Neptunium in LiCl-KCl Eutectic/Liquid Bismuth Systems", J. Electrochem. Soc., 147(2), 642 (2000).

[18] O. Shirai, K. Uozumi, T. Iwai, and Y. Arai, "Electrode reaction of the Np^{3+}/Np couple at liquid Cd and Bi electrodes in LiCl–KCl eutectic melts", J. Appl. Electrochem., 34(3), 323-330 (2004).

[19] O. Shirai, M. Iizuka, T. Iwai, and Y. Arai, "Electrode reaction of Pu^{3+}/Pu couple in LiCl-KCl eutectic melts: comparison of the electrode reaction at the surface of liquid Bi with that at a solid Mo electrode.", Anal. Sci., 17(1), 51-57 (2001).

[20] Y. Castrillejo, M.R. Bermejo, P.D. Arocas, A.M. Martínez, and E. Barrado, "The electrochemical behaviour of the Pr(III)/Pr redox system at Bi and Cd liquid electrodes in molten eutectic LiCl-KCl", J. Electroanal. Chem., 579(2), 343-358 (2005).

[21] Y. Castrillejo, M.R. Bermejo, P. Diaz Arocas, F. De la Rosa, and E. Barrado, "Electrode reaction of cerium into liquid bismuth in the eutectic LiCl-KCl", Denki Kagaku., 37(3), 636-643 (2005).

[22] Y. Castrillejo, R. Bermejo, A.M. Martínez, E. Barrado, and P. Díaz Arocas, "Application of electrochemical techniques in pyrochemical processes-Electrochemical behaviour of rare earths at W, Cd, Bi and Al electrodes", J. Nucl. Mater., 360(1), 32-42 (2007).

[23] M. Li, Q. Gu, W. Han, X. Zhang, Y. Sun, M. Zhang, and Y. Yan, "Electrochemical behavior of La(iii) on liquid Bi electrode in LiCl–KCl melts. Determination of thermodynamic properties of La–Bi and Li–Bi intermetallic compounds", RSC Adv., 5(100), 82471-82480 (2015).

[24] W. Han, N. Ji, J. Wang, M. Li, X. Yang, Y. Sun, and M. Zhang, "Electrochemical formation and thermodynamic properties of Tb–Bi intermetallic compounds in eutectic LiCl–KCl", RSC Adv., 7(50), 31682-31690 (2017).

[25] A.V. Volkovich, "Diffusion Coefficients of Alkaline-Earth Metal Ions in Molten Equimolar Mixtures of Potassium and Sodium Chlorides", Melts, 7(106), 43-43 (1993).

[26] M. Matsumiya, R. Takagi, and R. Fujita, "Recovery of EU^{2+} and Sr^{2+} using liquid metallic cathodes in molten nacl-kcl and kcl system", J. Nucl. Sci. Technol., 34(3), 310-317 (1997).

[27] M. Matsumiya, M. Takano, R. Takagi, and R. Fujita, "Recovery saof Ba^{2+} using liquid metallic cathodes in molten chlorides", J. Nucl. Sci. Technol., 35(11), 836-839 (1998).

[28] M. Matsumiya, M. Takano, R. Takagi, and R. Fujita, "Electrochemical Behavior of Ba^{2+} at Liquid Metal Cathodes in Molten Chlorides", Zeitschrift fur Naturforsch., 54(12), 739-746 (1999).

[29] M. Matsumiya, H. Matsuura, R. Takagi, and R. Fujita, "Continuous recovery of concentrated solute from the melt by countercurrent electromigration", J. Alloys Compd., 306(1-2), 87-95, (2000).

[30] M. Matsumiya and R. Takagi, "Electrochemical impedance spectroscopic study on Eu^{2+} and Sr^{2+} using liquid metal cathodes in molten chlorides", Zeitschrift fur Naturforsch. - Sect. A J. Phys. Sci., 55(8), 673-681 (2000).

[31] T. Lichtenstein, N.D. Smith, J. Gesualdi, K. Kumar, and H. Kim, "Thermodynamic properties of Barium-Bismuth alloys determined by emf measurements", Electrochim. Acta, 228, 628-635 (2017).

[32] J.M.P.Q. Delgado and M. Vazquez da Silva, "Analytical Solutions of Mass Transfer around a Prolate or an Oblate Spheroid Immersed in a Packed Bed", in Multiphase System and its Applications, Mohamed El-Amin, ed, 765-780, InTech, London (2011).

[33] D. Yoon, S. Phongikaroon, and J. Zhang, "Electrochemical and Thermodynamic Properties of $CeCl_3$ on Liquid Cadmium Cathode (LCC) in LiCl-KCl Eutectic Salt", J. Electrochem. Soc., 163(3), E97-E103 (2016).

[34] D. Yoon, "Electrochemical Studies of Cerium and Uranium in LiCl-KCl Eutectic for Fundamentals of Pyroprocessing Technology", Virginia Commonwealth University, Accessed Dec. 14 2016. Available from: https://scholarscompass.vcu.edu/cgi/viewcontent.cgi?article=5690&context=etd.

[35] A. Lasia, Electrochemical Impedance Spectroscopy and Its Applications, 1st ed., 143-248, Springer, New York (2014).

[36] D. Yoon and S. Phongikaroon, "Measurement and Analysis of Exchange Current Density for U/U^{3+} Reaction in LiCl-KCl Eutectic Salt via Various Electrochemical Techniques", Electrochim. Acta, 227, 170-179 (2017).